Accepted Manuscript

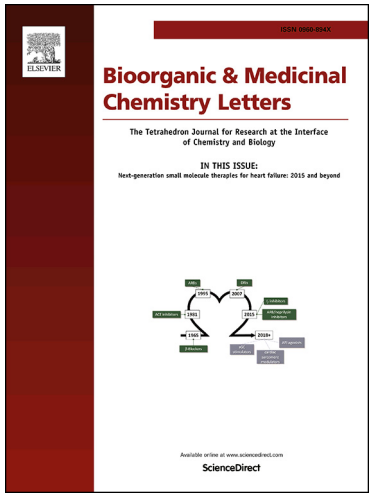

SAR inspired by aldehyde oxidase (AO) metabolism: Discovery of novel, CNS penetrant tricyclic M_4 PAMs

Trevor C. Chopko, Changho Han, Alison R. Gregro, Darren W. Engers, Andrew S. Felts, Mike S. Poslusney, Katrina A. Bollinger, Ryan D. Morrison, Michael Bubser, Atin Lamsal, Vincent B. Luscombe, Hyekyung P. Cho, Nathalie C. Schnetz-Boutaud, Alice L. Rodriguez, Sichen Chang, J. Scott Daniels, Donald F. Stec, Colleen M. Niswender, Carrie K. Jones, Michael R. Wood, Michael W. Wood, Mark E. Duggan, Nicholas J. Brandon, P. Jeffrey Conn, Thomas M. Bridges, Craig W. Lindsley, Bruce J. Melancon

PII: S0960-894X(19)30413-5
DOI: https://doi.org/10.1016/j.bmcl.2019.06.032
Reference: BMCL 26510

To appear in: *Bioorganic & Medicinal Chemistry Letters*

Received Date: 13 May 2019
Revised Date: 14 June 2019
Accepted Date: 19 June 2019

Please cite this article as: Chopko, T.C., Han, C., Gregro, A.R., Engers, D.W., Felts, A.S., Poslusney, M.S., Bollinger, K.A., Morrison, R.D., Bubser, M., Lamsal, A., Luscombe, V.B., Cho, H.P., Schnetz-Boutaud, N.C., Rodriguez, A.L., Chang, S., Scott Daniels, J., Stec, D.F., Niswender, C.M., Jones, C.K., Wood, M.R., Wood, M.W., Duggan, M.E., Brandon, N.J., Jeffrey Conn, P., Bridges, T.M., Lindsley, C.W., Melancon, B.J., SAR inspired by aldehyde oxidase (AO) metabolism: Discovery of novel, CNS penetrant tricyclic M_4 PAMs, *Bioorganic & Medicinal Chemistry Letters* (2019), doi: https://doi.org/10.1016/j.bmcl.2019.06.032

Graphical Abstract

To create your abstract, type over the instructions in the template box below.
Fonts or abstract dimensions should not be changed or altered.9.0_/0

SAR driven by aldehyde oxidase (AO) metabolism: Discovery of novel, CNS penetrant tricyclic M_4 PAMs

Leave this area blank for abstract info.

Trevor Chopko, Changho Han, Alison R. Gregro, Darren W. Engers, Andrew S. Felts, Mike S. Poslusney, Katrina A. Bollinger, Ryan D. Morrison, Michael Bubser, Atin Lamsal, Vincent B. Luscombe, Hyekyung P. Cho, Nathalie C. Schnetz-Boutaud, Alice L. Rodriguez, Sichen Chang, J. Scott Daniels, Donald F. Stec, Colleen M. Niswender, Carrie K. Jones, Michael R. Wood, Michael W. Wood, Mark E. Duggan, Nicholas J. Brandon, P. Jeffrey Conn, Thomas M. Bridges, Craig W. Lindsley and Bruce J. Melancon

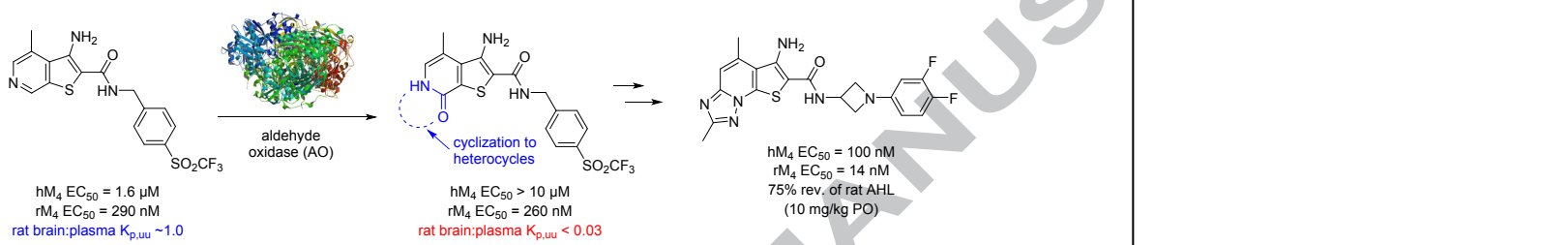

Bioorganic & Medicinal Chemistry Letters
journal homepage: www.elsevier.com

SAR inspired by aldehyde oxidase (AO) metabolism: Discovery of novel, CNS penetrant tricyclic M_4 PAMs

Trevor C. Chopko,[a†] Changho Han,[a†] Alison R. Gregro,[a] Darren W. Engers,[a,b] Andrew S. Felts,[a,b] Mike S. Poslusney,[a] Katrina A. Bollinger,[a] Ryan D. Morrison,[a] Michael Bubser,[a,b] Atin Lamsal,[a] Vincent B. Luscombe,[a] Hyekyung P. Cho,[a] Nathalie C. Schnetz-Boutaud,[a,b] Alice L. Rodriguez,[a,b] Sichen Chang,[a,b] J. Scott Daniels,[a,b,g] Donald F. Stec,[b,c,g] Colleen M. Niswender,[a,b,f,g] Carrie K. Jones,[a,b] Michael R. Wood,[a,b] Michael W. Wood,[e] Mark E. Duggan,[e] Nicholas J. Brandon,[e] P. Jeffrey Conn,[a,b,f,g] Thomas M. Bridges,[a,b] Craig W. Lindsley[a,b,c,d,g]* and Bruce J. Melancon[a,b]*

[a]*Vanderbilt Center for Neuroscience Drug Discovery, Vanderbilt University, Nashville, TN 37232, USA*
[b]*Department of Pharmacology, Vanderbilt University School of Medicine, Nashville, TN 37232, USA*
[c]*Department of Chemistry, Vanderbilt University, Nashville, TN 37232, USA*
[d]*Department of Biochemistry, Vanderbilt University, Nashville, TN 37232, USA*
[e]*AstraZeneca Neuroscience, IMED Biotech Unit, R&D Boston, MA 02451, USA.*
[f]*Vanderbilt Kennedy Center, Vanderbilt University School of Medicine, Nashville, TN 37232, USA*
[g]*Vanderbilt Institute of Chemical Biology, Vanderbilt University School of Medicine, Nashville, TN 37232, USA*

† *These authors contributed equally to this work.*
**To whom correspondence should be addressed: craig.lindsley@vanderbilt.edu or bruce.melancon@vanderbilt.edu*

ARTICLE INFO

Article history:
Received
Revised
Accepted
Available online

Keywords:
M_4
Muscarinic acetylcholine receptor
Positive allosteric modulator (PAM)
Structure-Activity Relationship (SAR)
Aldehyde oxidase (AO)

ABSTRACT

This letter describes progress towards an M_4 PAM preclinical candidate driven by an unexpected aldehyde oxidase (AO) metabolite of a novel, CNS penetrant thieno[2,3-*c*]pyridine core to an equipotent, non-CNS penetrant thieno[2,3-*c*]pyrdin-7(6*H*)-one core. Medicinal chemistry design efforts yielded two novel tricyclic cores that enhanced M_4 PAM potency, regained CNS penetration, displayed favorable DMPK properties and afforded robust *in vivo* efficacy in reversing amphetamine-induced hyperlocomotion in rats.

Positive allosteric modulators (PAMs) that act on the muscarinic acetylcholine receptor subtype 4 (M_4) continue to be the focus of programs developing new antipsychotic therapeutics, and other indications including Huntington's disease (HD) and Parkinson's disease (PD).[1-2, 5-7] In many of these studies, structure-activity relationships (SAR) of the thieno[2,3-*b*]pyridine 2-carboxamides and the thieno[2,3-*c*]pyridazine 6-carboxamides were derived from varied functionalization of these cores and driven by potency results from cell-based calcium efflux assays.[3-4] Recently, we have reported on our efforts to identify novel M_4 PAM chemotypes through scaffold hopping and a reexamination of hydrogen-bonding motifs contained within these privileged scaffolds.[8-23]Concurrent efforts also identified a series of ligands where an aldehyde oxidase (AO) metabolite of the thieno[2,3-*c*]pyridine 2-carboxamides drove the SAR towards new tricyclic analogues, culminating in the identification of a thieno[3,2-*e*][1,2,4]triazolo-[1,5-*a*]pyridine-7-carboxamide system. In this Letter, we report on the syntheses of these tricyclic ligands and their varied SAR and DMPK results that generated this novel class[25-27] of selective M_4 PAMs with excellent *in vitro* potency, good ADME properties, and one of the most pronounced reversals of amphetamine-induced hyperlocomotion (AHL) in an *in vivo* model reported for this class of compounds.

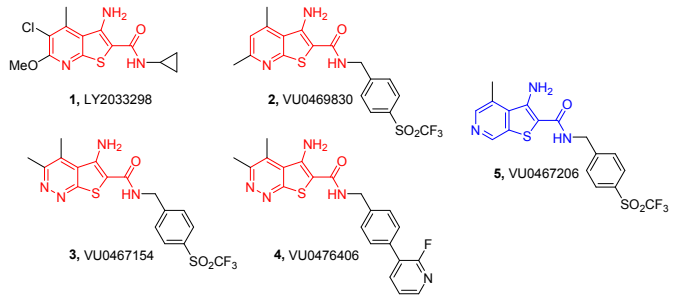

Figure 1. Historical M_4 PAMs showing a conserved ß-amino carboxamide (in red) with poor physicochemical properties. Compound **5** (VU0467206, in blue) has potential to improve solubility via salt formation.

While the dominant M_4 PAM chemotype is exemplified by either a thieno[2,3-*b*]pyridine 2-carboxamide or a thieno[2,3-*c*]pyridazine 6-carboxamide, these cores typically suffer from poor physicochemical properties and variable species muscarinic potency. To overcome solubility limited absorption, we explored other, related congeners with the potential for salt formation via a more basic nitrogen atom. Despite steep SAR that precluded the majority of targeted cores, a thieno[2,3-*c*]pyridine 2-carboxamide chemotype, exemplified by **5** (VU0467206), was identified as a novel M_4 PAM harboring a more basic nitrogen, with the potential to modulate physicochemical and DMPK properties.

The synthesis of **5** is illustrated in **Scheme 1**. Condensation of methyl 2-mercaptoacetate with isonicotinitrile **6** proceeds to provide **7** in 83% yield. Suzuki cross coupling reaction provides the 4-methylthieno[2,3-*c*]pyridine scaffold **8** in 56% yield. Saponification followed by HATU mediated coupling with the privileged trifluoromethylsulfone amine **9**, delivers compound **5** in 35% yield after reverse phase HPLC.

Scheme 1. Synthesis of thieno[2,3-*c*]pyridine M_4 PAM **5**.[a]

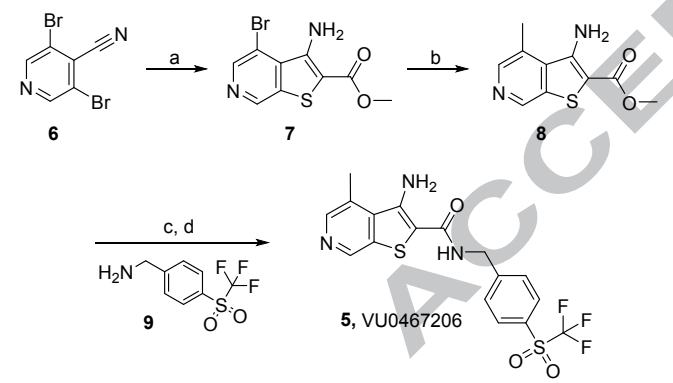

[a]Reagents and conditions: (a) methyl 2-mercaptoacetate, K_2CO_3, IPA, 65 °C, 83%; (b) CH_3-BF_3K, Pd(dppf)Cl_2·DCM, Cs_2CO_3, THF/H_2O (10:1), MW 145 °C, 56%; (c) aq. KOH, MeOH/H_2O (3:2), 50 °C, >99%; (d) R-NH_2, HATU, DIEA, DMF, rt, 35%.

Compound **5** proved to be a potent rat M_4 PAM (EC_{50} = 290 nM), but with a moderate to high predicted hepatic clearance (rat CL_{hep} = 51 mL/min/kg; rat microsomal CL_{int} = 200 mL/min/kg), which was confirmed *in vivo* (rat CL_p = 56 mL/min/kg), and thus a good in vitro/in vivo correlation (IVIVC). In our standard rat IV PBL cassette, **5** showed excellent brain penetration (brain:plasma K_p = 2.5, $K_{p,uu}$ = 1.0; 0.2 mg/kg, 10% EtOH, 40% PEG 400, 50% DMSO 2 mg/mL). Next, we dosed **5** in a discrete rat 10 mg/kg IP PBL study (10% Tween 80 in water, 4 mg/ mL) and observed similarly high CNS penetration (brain:plasma K_p = 1.8, $K_{p,uu}$ = 0.76). Encouraged by the potential of the thieno[2,3-*c*]pyridine core, we performed a metabolic soft-spot experiment in rat hepatic microsomes (+/- NADPH) to inform the rational design of analogs possessing increased metabolic stability. As shown in **Figure 2**, interestingly, we observed only minor

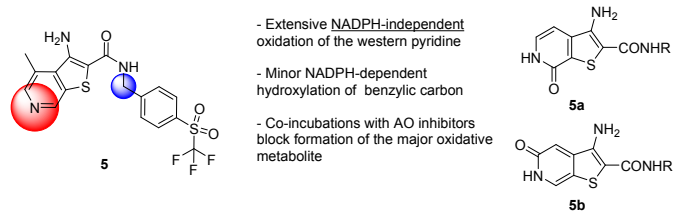

Figure 2. Soft-spot analysis of **5**. Confirmation of aldehyde oxidase-dependent (AO-dependent) metabolism was confirmed through AO inhibition *in vitro* suggesting either **5a** or **5b** as the core of the major AO metabolite.

NADPH-dependent metabolism (hydroxylation of the benzylic carbon), but noted extensive NADPH-independent oxidation of the western pyridine ring, later confirmed to be *via* aldehyde oxidase (AO). Based on previous experience with AO oxidation of heteroarenes,[24] we suspected that the major metabolite was either the thieno[2,3-*c*]pyridine-7(6*H*)-one **5a** or the thieno[2,3-*c*]pyridine-5(6*H*)-one **5b**.

After exhaustive 2D NMR experiments (^{1}H-^{1}H COSY, HSQC, HMBC), we identified the putative AO-mediated metabolite of M_4 PAM **5**, as the thieno[2,3-*c*]pyridine-7(6*H*)-one **5a** core, and specifically, compound **15** (VU6016365). We initiated the synthesis of compound **15** in order to independently confirm its structure. In **Scheme 2**, pyridone **10** was *bis*-brominated using *N*-bromosuccinimide to afford **11** and it was subsequently condensed with methyl thioglycolate to provide **12**. Protection of the penultimate aminothiophene with methoxymethyl chloride (MOMCl) proceeded in an efficient 56% yield over three steps, providing compound **13**. Saponification of the ester followed by standard amide coupling with our preferred amine provided compound **14** in good yield. Synthesis of the AO metabolite **15** was completed via palladium-mediated installation of the methyl group followed by removal of the hemi-aminal ether under aqueous acidic conditions.

Scheme 2. Synthesis of AO metabolite **15** (VU6016365).[a]

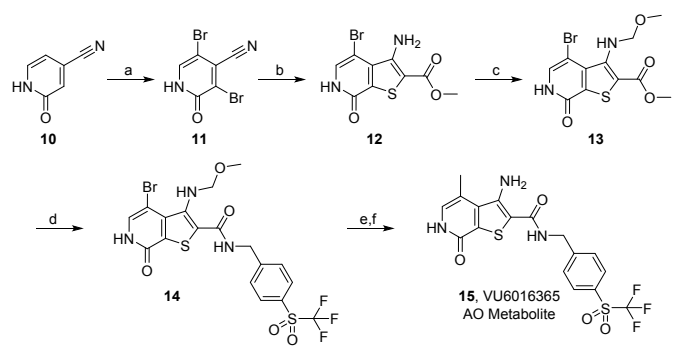

[a]Reagents and conditions: (a) NBS, ACN, 65 °C; (b) methylthioglycolate, K_2CO_3, IPA, 65 °C; (c) MOMCl, DIEA, DCM, 50 °C, 56% over 3 steps; (d) i. LiOH, THF/H_2O (3:2) 50 °C; ii. (4-((trifluoromethyl)sulfonyl)phenyl)methanamine, HATU, DIEA, DMF, rt, 31% over 2 steps; (e) CH_3BF_3K, Pd(dppf)Cl_2, Cs_2CO_3, 1,4-

dioxane/H_2O (10:1) 100 °C; (f) 4M HCl in 1,4-dioxane/H_2O, 85 °C, 3% over 2 steps.

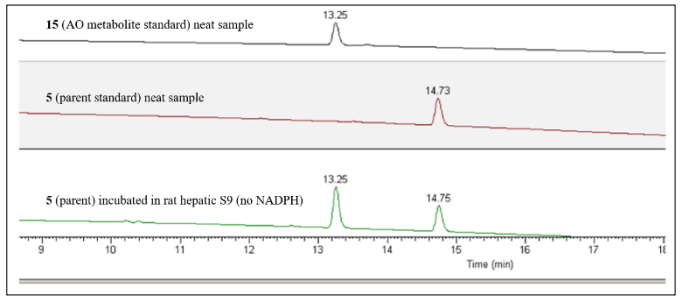

Figure 3. HPLC-UV (reverse phase) chromatograms of parent standard alone (**5**, retention = 14.7-14.8 min**)**, metabolite standard alone (**15**, retention = 13.2-13.3 min), and parent (**5**) incubated (25 µM, 1 hr, 37 ºC) in rat hepatic S9 (5 mg/mL, absence of NADPH).

With an authentic sample of **15** in hand, we compared the HPLC-UV chromatograms of the parent compound **5** to that of the AO metabolite **15** (**Figure 3**), and to compound **5** subjected to rat hepatic S9 incubation (without NADPH). There was excellent retention time correlation of the standards to the observed peaks from the hepatic S9 incubation. Confirmation of the metabolite identity was also provided by simultaneous mass spectrometric (MS^n) analysis, which revealed matching fragmentation patterns and ion spectra for the respective standards and S9 peaks. Further validation was then obtained by analysis of the sample from the S9 incubation after addition of the authentic standard of **15** (10 µM final concentration), which produced an increase in the corresponding peak area with the same MS^n spectra observed prior to addition. In light of these findings and the NMR data collected, we concluded that we had correctly identified the structure of **15**. Evaluation of the *in vitro* pharmacology of **15** showed it was similarly potent to **5** (rat M_4 EC_{50} = 260 nM) but had an increased fraction unbound in both rat and human plasma relative to **5** (**15**: human $f_{u\ plasma}$ = 0.024, rat $f_{u\ plasma}$ = 0.051), but was not centrally penetrant (brain:plasma K_p < 0.13, $K_{p,uu}$ < 0.03), likely as a result of an additional hydrogen bond donor conferring activity as a substrate for efflux transporter(s). While not a productive scaffold for CNS indications, we envisioned constraining the amide in **15** into five-membered heterocycles might maintain favorable properties while restoring CNS.

All of the potential tricyclic scaffolds required *de novo* syntheses. The first tricyclic series that we investigated mimicked the halogenation pattern of **1** (LY2033298, **Figure 1**). Starting with dichloropyridine (R_1 = H) or trichloropyridine (R_1 = Cl) **16**, S_NAr with sodium methanethiolate afforded compound **17** in good yield. Condensation with methyl thioglycolate, followed by saponification and amide coupling under standard conditions yielded a series of compounds with the generic structure of **19**. Oxidation of the sulfide to the sulfoxide **20** proceeded in moderate yield using hydrogen peroxide under acidic conditions. Treatment of **20** with hydrazine and triethylorthoacetate (R_2 = Me) or triethylorthoformate (R_2 = H) in one pot under microwave conditions produced a compound library of the structure **21**, **Scheme 3**.

Scheme 3. Synthesis of 1,3,4-triazole tricycles of **21**.[a]

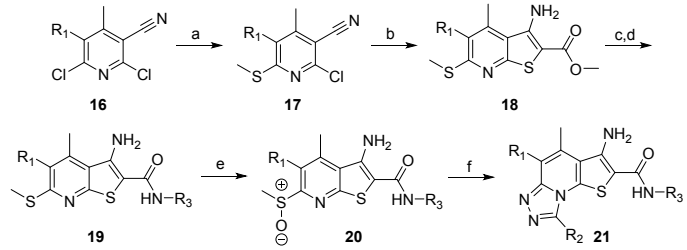

[a]Reagents and conditions: (a) NaSMe, MeOH, 91%; (b) methylthioglycolate, K_2CO_3, IPA, 50 °C, 65%; (c) KOH, H_2O, 100 °C, 98%; (d) R_3NH_2, HATU, DIEA, DMF, rt, 22-54%; (e) 30% H_2O_2, AcOH, 41%; (f) i. hydrazine hydrate, DMSO, MW 140 °C; ii. Triethylorthoformate or triethylorthoacetate, NMP, MW 180 °C, 21-53% over 2 steps.

The 1,3,4-triazolo tricyclic series of compounds (**Table 1**) was was separated into two classes where R_1 = H or R_1 = Cl. For compounds **21a-e**, we expected that R_1= Cl would be very potent M_4 PAMs as chloro-substituted methylpyridine scaffolds[1-23] were typically more potent than their proteo-counterparts: **21a** (EC_{50} = 16 nM), **21b** (EC_{50} = 12 nM), **21c** (EC_{50} = 20 nM), **21d** (EC_{50} = 22 nM), and **21e** (EC_{50} = 8 nM). However, despite their exquisite potency for the human M_4 receptor, these compounds exhibited low fraction unbound in brain homogenate (**21b**, rat $f_{u\ brain}$ = 0.002; **21c**, rat $f_{u\ brain}$ = 0.011) and many were substrates for P-gp efflux (MDCK-MDR1 cell line, efflux ratios from 5 to 73 for **21a-e**). Similarly, **21f-m** showed undesirable profiles with a 2-10 fold decrease in potency and high efflux ratios (MDCK-MDR1 cell line, efflux ratios > 15 for **21f-m**), which precluded their advancement.

Table 1. Structures and activities for M_4 PAM 1,3,4-triazole tricyclic analogs **21**.[a]

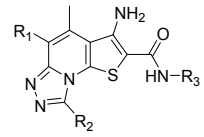

21

Cmpd	R_1	R_2	R_3	hM_4 EC_{50} (µM)[a] [% ACh Max]
15	-	-	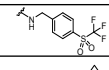	0.26 [84]
21a	Cl	H		0.016 [90]
21b	Cl	H	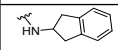	0.012 [82]
21c	Cl	H	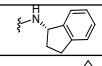	0.020 [73]
21d	Cl	CH_3		0.022 [88]
21e	Cl	CH_3	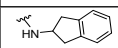	0.008 [94]
21f	H	H		0.11 [79]
21g	H	H	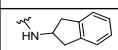	0.017 [87]
21h	H	H	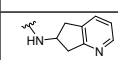	0.22 [84]
21i	H	H	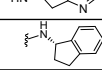	0.12 [71]
21j	H	H	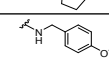	0.089 [78]
21k	H	H	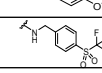	0.99 [60]
21l	H	H	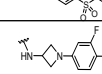	0.012 [84]
21m	H	H	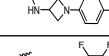	0.026 [87]

[a]For SAR determination, calcium mobilization human M_4/G_{qi5} assays were performed n = 1 independent times in triplicate with an EC_{20} fixed concentration of acetylcholine.

Undaunted, other tricyclic scaffolds were investigated, including the imidazo- and the 1,3,5-triazolo tricyclic variants. The synthesis of either scaffold began with dichloropyridine **22** (**Scheme 4,** panel **A**). Nucleophilic aromatic substitution with ammonia in methanol provided aminopyridine **23** with high regioselctivity in excellent yield. Condensation with methylthioglycolate at high temperature afforded diamino-4-methylthieno[2,3-*b*]pyridine **24**. In **Scheme 4**, panel **B**, the imidazo-tricyclic scaffold was constructed via condensation with chloroacetaldehyde or 1-chloropropan-2-one to provide either the unsubstituted hydrogen version or the methyl substituted congener **25**, (R_1 = Me or H). Saponification followed by amide coupling using HATU conditions provided a small library of compounds **26**. Similarly from compound **24**, 1,3,5-triazolo tricycles were synthesized via condensation with *N,N*-dimethylformamide dimethyl acetal or triethylorthoacetate in the presence of hydroxylamine. Cyclization/dehydration was accomplished using trifluoroacetic anhydride to afford **27**. Saponification with sodium hydroxide followed by amide coupling under standard HATU conditions provided a library of 1,3,5-triazolo tricycles **28**.

Scheme 4. Synthesis of tricyclic analogs **26** and **28**.[a]

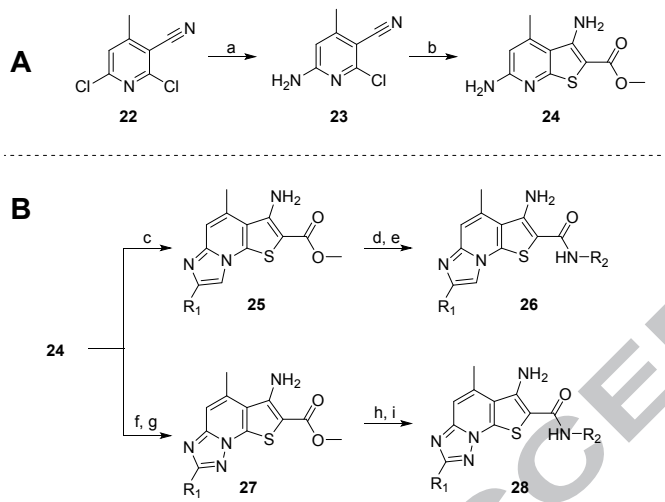

[a]Reagents and conditions: **Panel A.** Synthesis of diamino-4-methylthieno[2,3-b]pyridine **24**. Reagents and conditions: (a) 7 N NH_3 in MeOH, MW 150 °C, 90%; (b) methylthioglycolate, K_2CO_3, IPA, MW 120 °C, 51%. **Panel B.** Synthesis of imidazo-tricycles **26** and 1,3,5-triazolo tricycles **28**: (c) chloroacetaldehyde (R_1 = H) or 1-chloropropan-2-one (R_1 = Me), $NaHCO_3$, EtOH, 80 °C, 98%; (d) 6M NaOH, THF/MeOH (3:2), 53%; (e) R_2NH_2, HATU, DIEA, DMF, 18-43%; (f) DMF-DMA (R_1 = H) or triethylorthoacetate (R_1 = Me), $HONH_2$, IPA, 99%; (g) TFAA, THF, 0 °C, 90%; (h) NaOH, EtOH, 63%; (i) R_2NH_2, HATU, DIEA, DMF, 11-28%.

As shown in **Table 2**, imidazo-tricyclic analogs **26** proved to be less than optimal with a significant loss of potency compared to previous triazolo tricycles. While small alkyl amines (**26a**, EC_{50} = 130 nM) were still preferred, providing a potent compound, there were

Table 2. Structures and activities for M_4 PAM 1,3,4-triazolo tricyclic analogs **26**.[a]

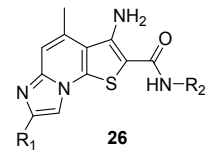

Cmpd	R_1	R_2	hM_4 EC_{50} (μM)[a] [% ACh Max]
26a	H		0.13 [77]
26b	H	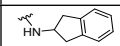	0.27 [80]
26c	H	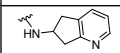	0.24 [66]
26d	H		2.1 [63]
26e	H	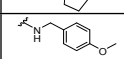	0.31 [65]
26f	CH_3	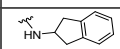	1.2 [76]
26g	CH_3	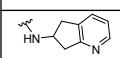	0.30 [71]
26h	CH_3		2.0 [47]

[a]For SAR determination, calcium mobilization human M_4/G_{qi5} assays were performed n = 1 independent times in triplicate with an EC_{20} fixed concentration of acetylcholine.

no compounds which were improved over previous library iterations with respect to potency (**26b-h**, EC_{50} s range from 240 nM to 2.1 μM).

Table 3 highlights the final tricyclic series investigated, the 1,3,5-triazolo tricycles. A limited set of unsubstituted triazoles (R_1 = H) was synthesized, **28a-28c**, with amides that possess good potency and were representative of well tolerated analogs across multiple scaffolds. These same amides were utilized in the substituted case (R_1 = Me) for compounds **28d-r**. Many compounds containing privileged M_4 PAM amides (**28d**, EC_{50} = 46 nM; **28e**, EC_{50} = 60 nM; **28g**, EC_{50} = 84 nM) had desirable potencies, but once again possessed poor physicochemical properties (xLogPs > 3.5). *N*-aryl-azetidine amides were previously reported to be potent analogs with the potential to be centrally penetrant. Here, compounds **28j-r** were synthesized and showed comparable potencies to previously described M_4 PAMs. **28j** is a moderately potent M_4 PAM (EC_{50} = 140 nM) with low *in vivo* clearance in rat (rat CL_p = 13 mL/min/kg); however, it suffered from low brain distribution (rat brain:plasma $K_{p,uu}$ = 0.02) and off-target activity at human muscarinic M_2 receptor (hM_2 EC_{50} = 650 nM). **28l** has similar properties to others in its series (hM_4 EC_{50} = 140 nM, rat CL_p = 13 mL/min/kg, rat brain:plasma $K_{p,uu}$ = 0.22, hM_2 EC_{50} > 10 μM), but ultimately suffered from relatively low brain penetration and poor physicochemical properties. Compound **28n** while a potent M_4 PAM, was also active at human M_2 (hM_2 EC_{50} = 600 nM), typifying the unpredictable SAR with respect to hM_2 for this series. Finally, **28p** is a potent M_4 PAM (hM_4 EC_{50} = 110 nM) and had low predicted clearance (rat CL_{hep} = 14 mL/min/kg based on microsomal CL_{int}), low *in vivo* clearance (rat CL_p = 15 mL/min/kg), and moderate brain distribution and low unbound brain concentration (rat brain:plasma K_p = 0.47, $K_{p,uu}$ = 0.04).[28] **28p** was evaluated in a bidirectional MDCK-MDR1 assay for its potential to be a substrate for human P-gp efflux and showed a low efflux ratio (ER = 1.2). While **28p** did show moderate potency at human M_2 (hM_2 EC_{50} = 1.2 μM), we chose to move it forward to

reversal studies of amphetamine-induced hyperlocomotion (AHL) in SD rats.

Table 3. Structures and activities for M_4 PAM 1,3,5-triazolo tricyclic analogs **28**.[a]

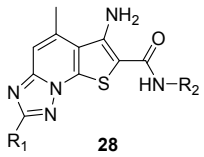

28

Cmpd	R_1	R_2	hM_4 EC_{50} (μM)[a] [% ACh Max]
28a	H	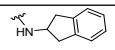	0.037 [85]
28b	H	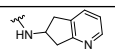	0.086 [76]
28c	H	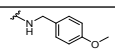	0.095 [80]
28d	CH_3	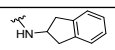	0.046 [80]
28e	CH_3	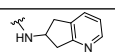	0.060 [75]
28f	CH_3	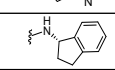	0.12 [63]
28g	CH_3	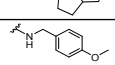	0.084 [84]
28h	CH_3	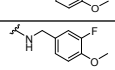	0.16 [90]
28i	CH_3	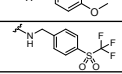	1.9 [56]
28j	CH_3	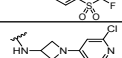	0.14 [89]
28k	CH_3	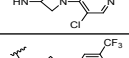	0.25 [90]
28l	CH_3	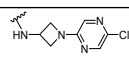	0.14 [91]
28m	CH_3	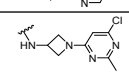	0.16 [94]
28n	CH_3	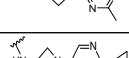	0.12 [86]
28o	CH_3	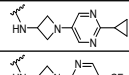	0.27 [87]
28p	CH_3	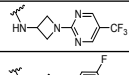	0.11 [91]
28q	CH_3	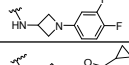	0.41 [97]
28r	CH_3	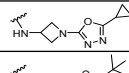	0.62 [86]

[a]For SAR determination, calcium mobilization human M_4/G_{qi5} assays were performed n = 1 independent times in triplicate with an EC_{20} fixed concentration of acetylcholine.

Compound **28p** (VU6001852) was formulated in 10% Tween 80 in water and dosed orally (10 mg/kg) in rats with 0.75 mg/kg (SC) challenge of amphetamine. When compared to control compound VU0467154, **28p** showed superior reversal of AHL at 75%, compared to 55% for the positive control (**Figure 4**). This is the largest reversal we have reported for this class of compounds. Overall, many of these tricyclic series had desirable potencies and DMPK properties but suffered from moderate activity at the M_2 receptor and some demonstrated P-gp efflux. Despite these liabilities, **28p** showed excellent reversal of AHL, and the promise of continued optimization of this novel series.

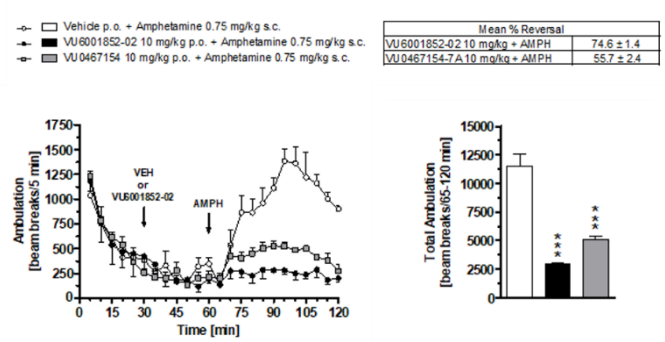

Figure 4. Reversal of amphetamine-induced hyperlocomotion in SD rats (male, $n \geq 4$ per dose group) by **28p** (VU6001852). M_4 PAM or vehicle (10% tween-80 90% water [v/v]) was administered orally 30 min after habituation in the chamber, and then 0.75 mg/kg amphetamine was administered subcutaneously 30 min later (t = 60 min). Total ambulations were measured over the subsequent 1 h interval (t = 60–120 min) and used to calculate % reversal of AHL for each dose group. Data represent means ± SEM and were analyzed by a one-way ANOVA; post hoc comparisons were made by Dunnett's test compared to amphetamine-vehicle conditions with statistical significance determined as $p < 0.05$.

In summary, we identified several novel tricyclic scaffolds with excellent potency at M_4, derived from a putative AO metabolite.[24] While some of the SAR data are reminiscent of our previous work highlighting the importance of certain structural motifs in the ß-amino carboxamide class of M_4 PAMs, there are disconnects based on the nature of the tricyclic core. Efforts towards development candidates in this, and other, novel scaffolds are underway, and will be reported in due course.

Acknowledgments

We thank the NIH and NIMH for funding (U19MH097056). We also thank William K. Warren, Jr. and the William K. Warren Foundation who funded the William K. Warren, Jr. Chair in Medicine (to C.W.L.).

References

1. A. Brady, C.K. Jones, T.M. Bridges, et al. *J. Phar. & Exp. Ther.* 327 (2008) 941.
2. W.Y. Chan, S. McKinzie, S. Bose, et al., *Proc. Natl. Acad. Sci. USA* 105 (2008) 10978.
3. J.P. Kennedy, T.M. Bridges, P.R. Gentry, et al., *ChemMedChem* 4 (2009) 1600.
4. J.M. Salovich, D.J. Sheffler. P.N. Vinson, et al., *Bioorg. Med Chem. Lett.* 22 (2012) 5084.
5. N.E. Byun, M. Grannan, M. Bubser, et al. *Neuropsychopharmacology* 39 (2014) 2693.
6. M. Bubser, T.M. Bridges, D.D. Thorek, et al. *ACS Chem. Neurosci.* 5 (2014) 920.
7. R.W. Gould, M.T. Nedelcovych, X. Gong, et al., *Neuropharmacology* 102 (2016) 244.
8. M.R. Wood, M.J. Noetzel, S. Takagi, et al., *Bioorg. Med Chem. Lett.* 26 (2016) 3029.
9. M.R. Wood, M.J. Noetzel, J.C. Tarr, et al., *Bioorg. Med Chem. Lett.* 26 (2016) 4282.
10. M.R. Wood, M.J. Noetzel, M.S. Poslunsey, et al., *Bioorg. Med Chem. Lett.* 27 (2017) 175.
11. M.R. Wood, M.J. Noetzel, B.J. Melancon, et al., *ACS Med Chem. Lett.* 8 (2017) 233.
12. B.J. Melancon, M.R. Wood, M.J. Noetzel, et al., *Bioorg. Med Chem. Lett.* 27 (2017) 2296.
13. C.J. Tarr, M.R. Wood, M.J. Noetzel, et al., *Bioorg. Med Chem. Lett.* 27 (2017) 2900.
14. C.J. Tarr, M.R. Wood, M.J. Noetzel, et al., *Bioorg. Med Chem. Lett.* 27 (2017) 5179.
15. R.W. Gould, M. Grannan, J. Ball, et al. *Neuropharmacology* 128 (2018) 492.

16. T. Huyn, C. Valant, I.T. Crosby, et al., *ACS Chem. Neurosci*. 6 (2015) 838.
17. D.J. Foster, J.M. Wilson, D.H. Remke, et al., *Neruon* 91 (2016) 1244.
18. M.S. Moehle, T. Pancani, N. Byun, et al., *Neuron* 96 (2017) 1358.
19. B.R. Bewley, P.K. Spearing, R. Weiner, et al. *Bioorg. Med. Chem. Lett.* 27 (2017) 4274.
20. M.F. Long, J.L. Engers, S. Chang, et al. *Bioorg. Med. Chem. Lett.* 27 (2017) 4999.
21. M.S. Poslusney, J.M. Salovich, M.R. Wood, et al. *Bioorg. Med. Chem. Lett.* 29 (2019) 362.
22. D.W. Engers, A.L. Blobaum, R.D. Gogliotti, et al. *ACS Chem. Neurosci*. 7 (2016) 1192.
23. T.T. Wager, X. Hou, P.R. Verhoest, A. Villalobos. *ACS Chem. Neurosci*. 7 (2016) 767.
24. A.S. Felts, A.L. Rodriguez, A.L. Blobaum, et al. *J. Med. Chem*. 60 (2017) 5072.
25. C.W. Lindsley, P.J. Conn, M.R. Wood, J.M. Salovich et. al. 2014, WO0364409.
26. P.J. Conn, C.W. Lindsley, M.R. Wood, et al. 2014, WO0357615.
27. C.W. Lindsley, P.J. Conn, D.W. Engers, et al. 2018, US 20180028501A1.
28. This measurement is based on a n = 1 for rat brain homogenate binding (rBHB). Efficacy in reversal of amphetamine-induced hyperlocomotion assays can be attributed to either total brain concentrations correlated to K_p or to unbound brain concentrations correlated to $K_{p,\,uu}$. Our program continues to evaluate which parameter is more important for in vivo efficacy in the context of M_4 . Compound **28p** has excellent reversal of AHL (75%) at 10 mg/kg, despite its low $K_{p,\,uu}$ = 0.04 and its moderate K_p = 0.47.